Letter

TiO2 Nanotube Arrays Modified Titanium: A Stable, Scalable, and Cost-Effective Bioanode for Microbial Fuel Cells

Huajun Feng, Yuxiang Liang, Kun Guo, Wei Chen, Dongsheng Shen, Lijie Huang, Yuyang Zhou, Meizhen Wang, and Yuyang Long

Environ. Sci. Technol. Lett., **Just Accepted Manuscript** • DOI: 10.1021/acs.estlett.6b00410 • Publication Date (Web): 21 Nov 2016

TiO_2 Nanotube Arrays Modified Titanium: A Stable, Scalable, and Cost-Effective Bioanode for Microbial Fuel Cells

Huajun Feng[†], Yuxiang Liang[†], Kun Guo[†‡*], Wei Chen[†], Dongsheng Shen[†], Lijie Huang[†], Yuyang Zhou[†], Meizhen Wang[†], Yuyang Long[†*].

[†] *Zhejiang Provincial Key Laboratory of Solid Waste Treatment and Recycling, School of Environmental Science and Engineering, Zhejiang Gongshang University, Hangzhou 310012, China;*

[‡] *Center for Microbial Ecology and Technology, Ghent University, Coupure Links 653, B-9000, Ghent, Belgium*

* *Corresponding author:*

Yuyang Long: Zhejiang Provincial Key Laboratory of Solid Waste Treatment and Recycling, School of Environmental Science and Engineering, Zhejiang Gongshang University, Hangzhou 310012, China. longyy@zjgsu.edu.cn; Phone: +86 571 87397126

Kun Guo: E-mail address: Center for Microbial Ecology and Technology, Ghent University, Coupure Links 653, B-9000, Ghent, Belgium. kun.guo@ugent.be; Phone: +32 (0)9 264 59 85

TOC Art:

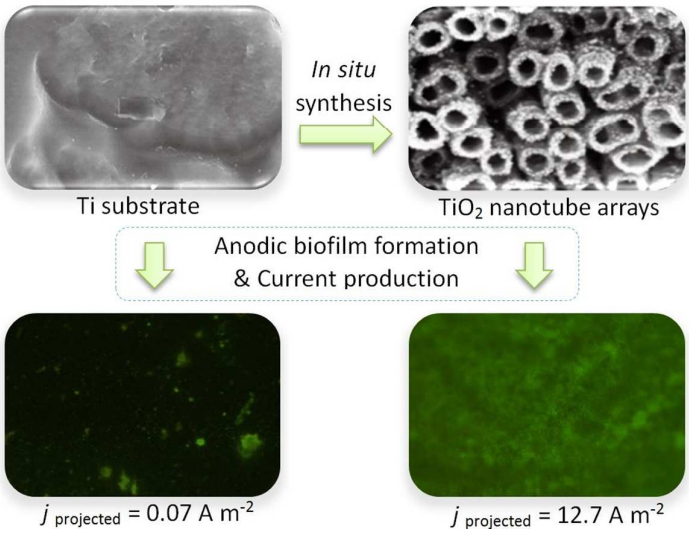

Abstract:

Titanium has been widely used as a dimensionally stable anode in the electrolysis industry because of its excellent corrosion–resistance, conductivity, and scalability. However, due to its poor biocompatibility and low performance as bioanode, it has drawn little attention in the field of microbial fuel cells (MFCs). This study reports an efficient way to convert titanium electrode into a high-performance anode for MFCs, *in-situ* growth of titanium dioxide nanotubes (TNs) on its surface. After TNs modification, the titanium surface became rougher, more hydrophilic, and more conducive for anodic biofilm formation. The maximum current density achieved on this TNs-modified titanium electrode was 12.7 A m^{-2}, which was 190-fold higher than the bare Titanium electrode and even higher the most-commonly used carbon felt electrode. Therefore, the high conductivity, corrosion-resistance, and current density make TNs-modified titanium electrode a promising and scalable anode for MFCs.

INTRODUCTION

Microbial fuel cell (MFC) is an emerging technology that can directly convert organic waste into electrical energy through the metabolism of electrochemically active microorganisms (EAMs).[1] In past decades, remarkable improvements have been achieved in MFCs in terms of increasing power/current density, finding new electrode materials, optimizing reactor configurations, and understanding EAMs. However, scaling this technology for practical application is still limited by low power density and high capital cost. The electrodes are the core components that determine the cost and the performance of MFCs. Thus, finding cost-effective electrode materials has drawn increased recent attention and a variety of novel electrodes have been reported.[2]

Due to their excellent biocompatibility and chemical stability, carbon-based electrodes in various configurations (e.g. paper, cloth, felt, foam, brush) have been extensively used in MFCs.[3] However, their low electrical conductivity and mechanical strength remain major obstacles for their practical application at larger scale. Consequently, metal-based electrodes, such as gold, silver, copper, nickel, cobalt, stainless steel, and titanium, have been recently tested as anodes.[3-8] Among these metals, copper and stainless steel are considered as the most promising anode materials as they are relative cheap, scalable, and producing comparable current density to that of graphite electrode.[4,8] However, the relative low corrosion resistance of copper and stainless steel means that they cannot be used in an uncontrolled wastewater treatment environment (e.g. high concentration of ammonia nitrogen, salinity, oxidant and hydrogen ions) but, rather, have to be used in a well-controlled environment (e.g. more reducing environment).[9] Therefore, it is still of great importance to find stable and cost-effective metal-based electrodes for MFCs.

Titanium has been widely used as a dimensionally stable anode in the electrolysis industry because of its excellent corrosion resistance, mechanical properties, and electric conductivity.[10,11] However, in previous studies, the performance of titanium as

anode of MFCs was so poor that it was mainly used as current collectors for carbon electrodes. The prior poor performance of titanium anodes in MFCs is likely because the passive layer on titanium makes them unfavorable for EAM biofilm formation and inhibits electron transfer between microorganisms and the electrode.[4, 12] Hence, surface modification of titanium with biocompatible materials might be an effective way to convert it into a high-performance anode for MFCs. TiO_2 nanoparticles are biocompatible and stable, and recently have been used to modify carbon electrode to improve the power output of MFCs.[13,14] Moreover, it has been reported that TiO_2 nanotube can be in-situ synthesized used as an adhesion support platform for bone and stem cells.[13] Therefore, the aim of this study was to synthesize TiO_2 nanotube arrays on a titanium plate surface and to test the performance of the modified titanium electrode as a bio-anode in MFCs.

MATERIALS AND METHODS

Preparation of TiO_2 nanotube arrays

A Ti plate (purity, 99.6%, Guangzhou China; thickness 0.5 mm) was cut into 1.0 cm × 2.0 cm pieces. Before modification, the Ti plates were sequentially cleaned in acetone, ethanol and deionized (DI) water by ultrasonication for 30 min. The TiO_2 nanotube arrays were synthesized on the cleaned Ti plates by anodic oxidation in 5 wt. % NaF electrolyte (ethylene glycol/H_2O = 8:2) following the method described in an earlier report.[13] The procedure of the treatment was summarized in Fig. S1. Briefly, the Ti plate was electrochemically oxidized in 5 wt. % NaF electrolyte (ethylene glycol/H_2O = 8:2) in a two-electrode setup with another Ti plate (two times bigger than the anode) as the counter electrode. The voltage was held at 30 V for 6 h and the temperature of the electrolyte was maintained at 55 °C. After that, the modified Ti plates were ultrasonically cleaned in deionized (DI) water for 30 s. Finally, the Ti plates were annealed in a muffle furnace at 450 °C for 2 h to obtain an anatase structure.

Characterization of TiO_2 nanotube arrays

The surface morphology of the anode was characterized using a field emission scanning electron microscope (FESEM; SU-70, Hitachi, Japan). The surface chemical composition was measured using X-ray photoelectron spectroscopy (XPS), which was collected using an EscaLab 250Xi spectrometer with a monochromated Al Kα source (Thermo, England). Spectra were calibrated on the Ti and O element and analyzed using XPSPEAK41 software. The static water contact angles of the hybrid membranes were determined by using a contact angle goniometer (DSA100, Krüss, Germany).

Electrochemical characterization of TiO_2 nanotube arrays

All electrochemical measurements were performed using an electrochemical workstation (Biologic VSP, Claix, France) in a three-electrode cell. All potentials in this work are quoted relative to the Ag/AgCl (3.5 M KCl) reference electrode. The EIS measurements were performed at an open circuit potential, amplitude of 10 mV, and a frequency range of 100 kHz to 1 Hz in sterile M9 solution. The corrosion potential was recorded by linear sweep voltammetry (LSV) in sterile M9 solution. The potential window was −0.8 to 0.2 V and the scan rate was 0.1 mV s^{-1}.

Reactor construction

All electrodes were tested in a cylindrical and dual-chamber reactor, as shown in detail in Fig. S2A. This reactor contained eight anodes with one cathode. The volume of the anodic chamber was 800 mL and that of the cathodic chamber was 100 mL. For TiO_2 nanotube arrays modification, we used four parallel electrodes that were placed on opposite sides of the reactor. For other modifications, we used two parallel electrodes. The compartments were separated by a cation exchange membrane (CMI-7000, Membranes International, USA), which was immersed in 5% NaCl solution for 24 h before use. All reactors were cultivated at a stable ambient temperature (40±2 °C) controlled by a thermotank. The anolyte consisted of CH_3COONa (1 g/L), M9 solution (NH_4Cl, 0.1 g/L; NaCl, 0.5 g/L; KH_2PO_4, 4.4 g/L; K_2HPO_4, 3.4 g/L; $MgSO_4$, 0.1 g/L; $NaHCO_3$, 2 g/L) and trace elements.[20] The anolyte was inoculated with 100 mL fresh anodic effluent (OD600 was about 1) of an existing acetate-fed MFC reactor in the lab that had been continuously running for

two years. The catholyte was 20 g/L $K_3[Fe(CN)_6]$. The external resistance was 1 Ω (Fig. S2B) and the current generation data were collected using a data acquisition instrument (34970A, Agilent, USA). All average current densities were calculated based on the data from day 4-8.

Characterization of the biofilm

Current data were collected using a data acquisition instrument (34970A, Agilent, USA). Biofilm CV was performed within −0.8 to 0.2 V at a scan rate of 1 mV s^{-1} in fresh anolyte. EIS was measured at an open circuit potential. The frequency ranged from 1 kHz to 1 mHz and the polarization potential was 10 mV in fresh anolyte. After acclimation for 20 days, the biofilm samples of two pieces were subjected to the LIVE/DEAD BacLight bacterial viability test (LIVE/DEAD® BacLight™ Bacterial Viability Kit, Molecular Probes, USA) and captured using a fluorescence microscope (DM2500, Leica, Germany). The biofilm samples of another two pieces were subjected to cell disruption and then used to measure the protein concentration using the Folin's phenol reagent methods. [15]

RESULTS AND DISCUSSION

Evaluation of electrode performance

The surface of the Ti substrate (TS) was silvery gray and shiny. After synthesis of the TiO_2 nanotube arrays (TNs), the color of surface became violet and lost its metallic luster. SEM images (Fig. 1B-F) showed that the surface of the Ti substrate was densely packed with a wave texture, whereas the TNs was neatly covered with nanoscale tubes (diameter: 60–90 nm; wall thickness: ~20 nm) which resulted in an increased surface area of the electrode. In addition, the Ti substrate turned blue only after heat treatment at 450 °C for 2 h (HT) and its surface structure was similar to that of TS, indicating that very thin titanium oxide layers were formed (Fig. S3).

High-resolution XPS scans of the Ti and O regions are shown in Fig. 1G. All of the electrodes exhibited two peaks (Ti^{4+}-1/2p and Ti^{4+}-3/2p) at binding energies of 458.7 and 465.1 eV, respectively, [16,17] which indicated that the surface titanium of HT and

TNs was completely oxidized and formed a layer of titanium oxide. A different peak of Ti^0 at 454.6 eV was observed on TS, which indicated that the surface titanium was oxidized in air. However, this only occurred to a limited extent on pristine titanium. In addition, the O1s XPS spectra of TNs and HT also showed a single clear peak of Ti–O=O at 531.3 eV, whereas different peaks at 530.4 (Ti–OH) and 532.8 eV (Ti–O) were observed on the surface of TS, which may be attributed to the water adsorbed on the surface.[18]

The XPS results showed that the surfaces of TNs, HT and TS had a similar chemical composition. Therefore, the increase in capacitance is consistent with the increase of the BET surface area.[6] Based on electrochemical impedance spectroscopy (EIS) in a sterile M9 medium (Fig. S4), the surface capacitance of the TNs increased from 0.043 to 0.462 mF cm^{-2}, which means that the effective contact areas with the water of TNs were at least 10-fold higher than that of TS. In addition, the water contact angle of the TS was greater than 120° (Fig. S3B). After anodic oxidation, the water droplet promptly integrated into the TNs electrode, indicating that the hydrophobic metal surface was transformed into a hydrophilic surface in the TiO_2 nanotube arrays.

Current generation and biofilm characterization

The power output performance of TNs was tested in a cylindrical and dual-chamber reactor. Fig. 2A and S5 shows the current generation over time for the TNs, HT and TS. After 4 days of operation, the maximum projected current density ($j_{projected}$) of TNs was 12.7 ± 0.7 A m^{-2} (mean ± SD, n=3), which was more than 190-fold higher than that of TS (0.07 ± 0.02 A m^{-2}, n=2). In addition, HT only showed a small increase in current output (0.16 ± 0.03 A m^{-2}, n=2), indicating the contribution of heat treatment to the enhancement of current output was very limited.

Cyclic voltammetry of the biofilm was conducted in the same medium to investigate the electrochemical activity (Fig. 2B). Compared with the electrode CVs in bare M9 medium (Fig. S6), the biofilm CVs of the TNs exhibited a classic

sigmoidal shape under acetate turnover conditions, indicating that the generation of the current could be attributed to biofilm-associated extracellular electrons.[6]

Biofilms were visualized using fluorescence microscopy (Fig. 2C). The image showed that the live bacteria biofilms covered 100% of the surface of the TNs, while almost no biofilm was attached to the surface of TS and HT. Similarly, the protein concentration (583 ± 55 μg cm^{-2}) on TNs was approximately 15 times higher than that of the TS (38 ± 12 μg cm^{-2}) (Fig. S7). Next, we performed EIS at an open circuit potential of the biofilm (~−460 mV) to measure the charge transfer process between the anode and the biofilm. As shown in Fig. 2D, the charge transfer resistance (R_{ct}) of TNs was ~580 Ω, compared with ~14,800 Ω for HT and ~28,600 Ω for TS. This improvement in resistance may be caused by the high conductive contact area between biofilm and TNs.[19] In summary, these results indicated that the TiO_2 nanotubes were suitable for biofilm formation.

Comparison with other high-performance anode materials

Prior reports of MFCs with titanium plate anodes have shown an extremely low current output (range from 0 to 0.0006 A m^{-2}; see Table 1).[4,12] The maximum current density achieved in this study is much higher than these previous reports. It is somewhat complex to compare the current densities among different researches because the reactor designs, medium compositions, microbial inoculum, and operational conditions are different in different research groups. However, most-commonly used graphite plate (6.0 ± 0.6 A m^{-2}, n=2) and graphite felt (11.3 ± 0.4 A m^{-2}, n=2) were also tested under the same conditions in this study (Fig. S8), and the maximum current densities achieved on them were all lower than that of TNs ($p < 0.05$), indicating that TNs was indeed a high performance anode material for MFCs.

Furthermore, the current output of TNs is also higher than that produced by other metal electrodes, such as copper, nickel, silver and gold plate electrodes. Gold and silver don't require a detailed analysis of the performance because those noble metals are cost-prohibitive in practical applications. Copper and stainless steel (SS) are

commercially available on a large scale. However, these metals are susceptible to corrosion under the influence of certain ions, such as chloride from M9 solution.,[4] When exposed to M9, the corrosion potential of these metals became more negative (copper: −0.26 V, stainless steel: −0.55 V) (Fig. S9). This propensity to corrosion would inhibit their development as bio-anodes. By comparison, titanium has the most positive corrosion potential (−0.08 V in sterile solution; −0.10 V under the presence of biofilm).

Additionally, table 1 also shows the comparisons of the prices of some high performance materials. Titanium plate is commercially available at larger scale, and its price (30 k$ m^{-3}) is similar to graphite felt (25-75 k$ m^{-3}). The lowest material costs (21 k$ m^{-3}) is SS electrode, while since SS foam (830 – 1600 k$ m^{-3}) and SS felt (30 – 100 k$ m^{-3}) are not widely circulated in the market, the prices of them are much higher than titanium. In summary, TNs has a high conductivity, corrosion-resistance, and low price, improving its comparative benefit in real-world applications as a bio-anode.

ASSOCIATED CONTENT

Supporting Information

The Supporting Information is available free of charge on the ACS Publications website.

The preparation of TiO_2 nanotube arrays (Fig. S1), schematic of the MFCs reactor setup (Fig. S2), additional SEM images (Fig. S3), and all data collected form electrode and biofilm samples (Fig. S4-S9).

AUTHOR INFORMATION

Corresponding authors

E-mail address: longyy@zjgsu.edu.cn; Phone: +86 571 87397126

E-mail address: kun.guo@ugent.be; Phone: +32 (0)9 264 59 85

235

236 **Notes**

237 The authors declare no conflict of interest.

238

239 **ACKNOWLEDGEMENTS**

240 This work was supported by the National Natural Science Foundation of China
241 (51478431) and the Public Technology Research Plan of Zhejiang Province
242 (2014C33028).

243

244 **References**

245 1 Logan, B. E.; Rabaey, K. Conversion of wastes into bioelectricity and chemicals by
246 using microbial electrochemical technologies. *Science* **2012**, *337*, 686−690.
247 2 Xie, X.; Cridddle, C.; Cui, Y. Design and fabrication of bioelectrodes for microbial
248 bioelectrochemical systems. *Energy Environ. Sci.* **2015**, *8*, 94−113.
249 3 Guo, K.; Prévoteau, A.; Patil, S. A.; Rabaey, K. Engineering electrodes for microbial
250 electrocatalysis. *Curr. Opin. Biotech.* **2015**, *33*, 149−156.
251 4 Baudler, A.; Schmidt, L.; Langner, M.; Greiner, A.; Schroder, U. Does it have to be
252 carbon? Metal anodes in microbial fuel cells and related bioelectrochemical systems.
253 *Energy Environ. Sci.* **2015**, *8*, 2048−2055.
254 5 Liang, Y. X.; Feng, H. J.; Shen, D. S.; Long, Y. Y.; Li, N.; Zhou, Y. Y.; Ying, X. B.;
255 Gu, Y.; Wang, Y. F. Metal-based anode for high performance bioelectrochemical
256 systems through photo-electrochemical interaction. *J. Power Sources* **2016**, *324*,
257 26−32.
258 6 Guo, K.; Donose, B. C.; Soeriyadi, A. H.; Prévoteau, A.; Patil, S. A.; Freguia, S.;
259 Gooding, J. J.; Rabaey, K. Flame oxidation of stainless steel felt enhances anodic
260 biofilm formation and current output in bioelectrochemical systems. *Environ. Sci.*
261 *Technol.* **2014**, *48*, 7151−7156.
262 7 Guo, K.; Soeriyadi, A. H.; Feng, H. J.; Prévoteau, A.; Patil, S. A.; Gooding, J. J.;
263 Rabaey, K. Heat-treated stainless steel felt as scalable anode material for

bioelectrochemical systems. *Bioresource Technol.* **2015**, *195*, 46−50.

8 Ketep, S. F.; Bergel, A.; Calmet, A.; Erable, B. Stainless steel foam increases the current produced by microbial bioanodes in bioelectrochemical systems. *Energy Environ, Sci.* **2014**, *7*, 1633−1637.

9 Otmačić, H.; Stupnišek-Lisac, E. Copper corrosion inhibitors in near neutral media. *Electrochim. Acta* **2003**, *48*, 985−991.

10 Charriere, R.; Lacaille, G.; Pedeferri, M. P.; Faucheu, J.; Delafosse, D. Characterization of the gonioapparent character of colored anodized titanium surfaces, *Color Res. Appl.* **2015**, *40*, 483−490.

11 Ohtsu, N.; Kozuka, T.; Hirano, M.; Arai, H. Electrolyte effects on the surface chemistry and cellular response of anodized titanium. *Appl. Surf. Sci.* **2015**, *349*, 911−915.

12 Zhou, X. W.; Chen, X. F.; Li, H. Y.; Xiong, J.; Li, X. P.; Li, W. S. Surface oxygen-rich titanium as anode for high performance microbial fuel cell. *Electrochim. Acta* **2016**, *209*, 582−590.

13 Zhang, J.; Liu, L. Z.; Yang, L.; Gan, Z. X.; Wu, X. L.; Chu, P. K. 3C-SiC nanocrystals/TiO_2 nanotube heterostructures with enhanced photocatalytic performance. *Appl. Phys. Lett.* **2014,** *104,* 231902.

14 Paulose, M.; Prakasam, H. E.; Varghese, O. K.; Peng, L.; Popat, K. C.; Mor, G. K.; Desai, T. A.; Grimes, C. A. TiO_2 nanotube arrays of 1000 μm length by anodization of titanium foil: Phenol red diffusion. *J. Phys. Chem. C* **2007**, *111*, 14992−14997.

15 Lowry, O. H.; Rosebrough, N. J.; A. Farr, L.; Randall, R. J. Protein measuremrnt with the folin-Phenol reagent. *J. Biol. Chem.* **1951**, *193*, 265−275.

16 Georgiadou, I.; Spanos, N.; Papadopoulou, C.; Matralis, H.; Kordulis, C.; Lycourghiotis, A. Preparation and Characterization of Various Titanias (anatase) used as Supports for Vanadia. *Colloid Surf. A* **1995**, *98*, 155−165.

17 Sullivan, J. L.; Saied, S. O.; Xu, N. S. Effect of ion and neutral sputtering on single crystal TiO_2. *Vacuum*, 1991, **42**, 849–862.

18 Ingo, G. M.; Dire, S.; Babonneau, F. XPS studies of SiO_2-TiO_2 powders prepared by sol-gel process. *Appl. Surf. Sci.* **1993**, *70*, 230–234.

19 Feng, H. J.; Liang, Y. X.; Guo, K.; Li, N.; Shen, D. S.; Cong, Y. Q.; Zhou, Y. Y.; Wang, Y. F.; Wang, M. Z.; Long, Y. Y.; Hybridization of photoanode and bioanode to enhance the current production of bioelectrochemical systems. *Water Res.*, 2016, **102**, 428–435.

20 Zheng, S. Q.; Yang, F. F.; Chen, S. L.; Liu, L.; Xiong, Q.; Yu, T.; Zhao, F.; Schroder, U.; Hou, H. Q. Binder-free carbon black/stainless steel mesh composite electrode for high-performance anode in microbial fuel cells. *J. Power Sources* **2015**, *284*, 252–257.

21 Ketep, S. F.; Bergel, A.; Calmet, A.; Erable, B. Stainless steel foam increases the current produced by microbial bioanodes in bioelectrochemical systems. *Energy Environ, Sci.* **2014**, *7*, 1633–1637.

22 Pocaznoi, D.; Calmet, A.; Etcheverry, L.; Erable, B.; Bergel, A. Stainless steel is a promising electrode material for anodes of microbial fuel cells. *Energy Environ. Sci.* **2012**, *5*, 9645–9652.

23 Hou, J. X.; Liu, Z. L.; Yang, S. Q.; Zhou, Y. Three-dimensional macroporous anodes based on stainless steel fiber felt for high-performance microbial fuel cells. *J. Power Sources* **2014**, *258*, 204–209.

24 Erbay, C.; Pu, X.; Choi, W.; Choi, M. J.; Ryu, Y.; Hou, H. J.; Lin, F.; Figueiredo, P.; Yu, C.; Han, A. Control of geometrical properties of carbon nanotube electrodes towards high-performance microbial fuel cells. *J. Power Sources* **2015**, *280*, 347–354.

25 Guo, K.; Hidalgo, D.; Tommasi T.; Rabaey K. Pyrolytic carbon-coated stainless steel felt as a high-performance anode for bioelectrochemical systems. *Bioresource Technol.* **2016**, *211*, 664−668.

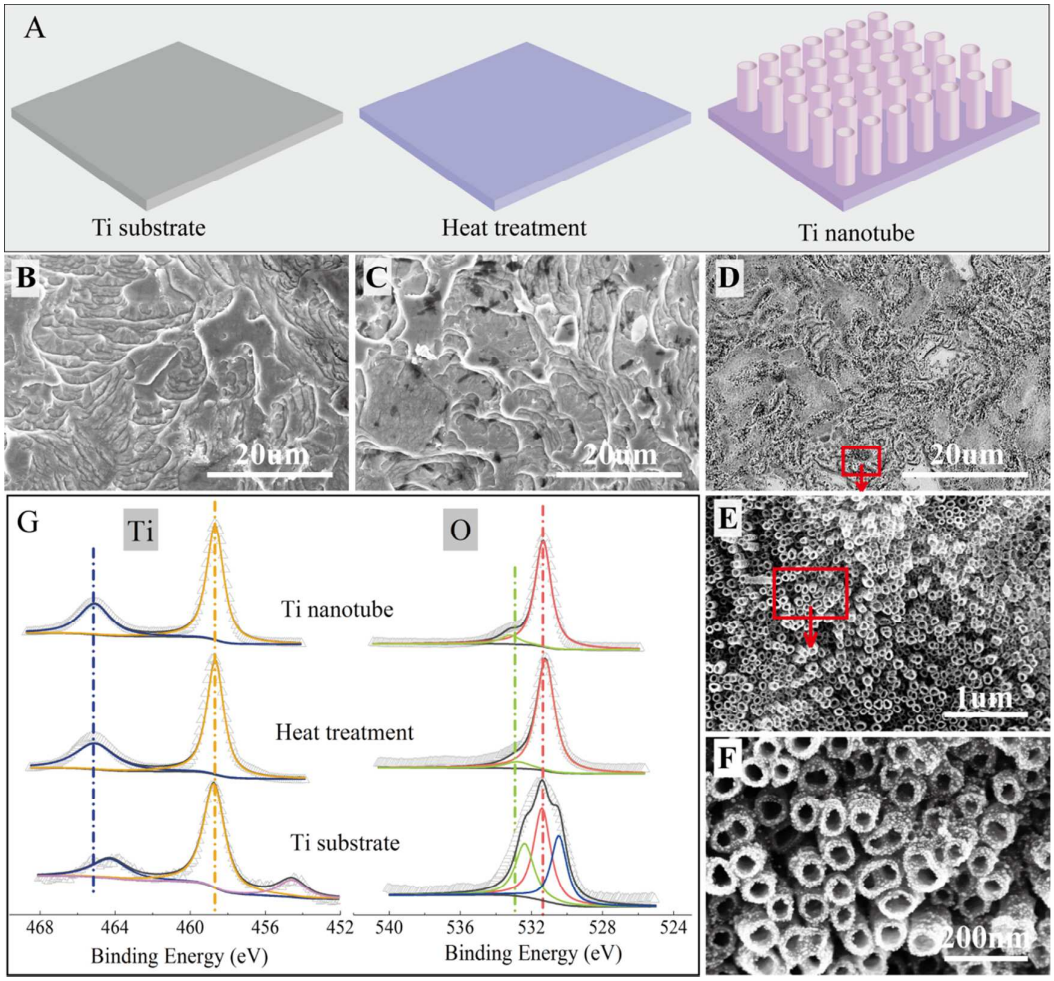

Fig. 1 (A–D) Schematic illustration and SEM images for the Ti substrate after different treatments: Ti substrate (A, B), heat treatment (A, C) and Ti nanotube (A, D); (E, F) Partial enlarged detail SEM images for the Ti nanotube; (G) XPS characterization: Ti region and O region. Blue and orange lines refer to Ti^{4+}-1/2p and Ti^{4+}-3/2p, respectively. Red and green lines refer to Ti–O=O and Ti–O, respectively.

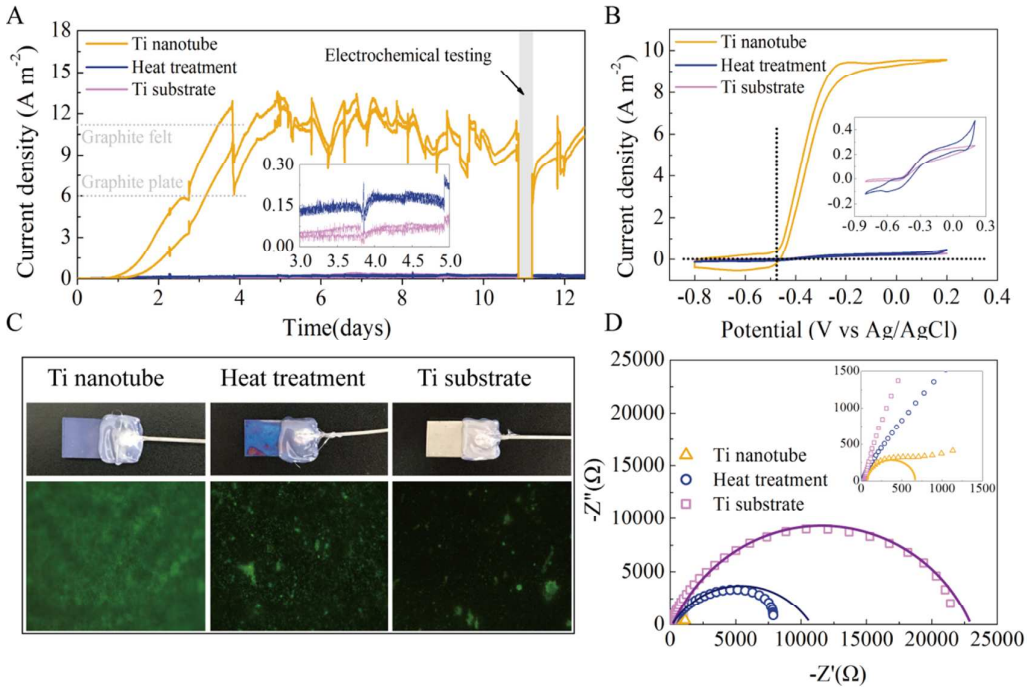

325

326 Fig. 2 (A) Current output over time of MFCs with different anodes (the data of
327 graphite electrodes showed in Fig. S4). (B) Cyclic voltammetry (1 mV/s) response of
328 the anode in fresh culture. The CVs were obtained starting from the second cycle. (C)
329 Fluorescence microscopy of the biofilms on different electrodes. The biofilms were
330 stained using the LIVE/DEAD Bac-Light bacterial viability kit (live bacteria, green).
331 (D) Electrochemical impedance spectroscopy for the biotic Ti substrate after different
332 treatment at open circuit potential, an amplitude of 10 mV, and a frequency range of 1
333 kHz to 1 mHz in fresh culture.

334

335 Table 1 Summary of high-performance metal bio-anodes in MFCs

Metal electrodes for BESs	$j_{projected}$ [a] ($A\ m^{-2}$)	Price [b] ($k\$\ m^{-3}$)	Corrosion potential (V) [c]	Ref
Carbon black/SS	101	/	/	20
SS foam	82	830-1600 [e]	/	21
254SMO SS grade	22	/	/	22
Flame oxidation SS felt	19	/	/	6
Heat-treated SS felt	15	30-100 [e]	/	7
Copper electrode [d]	15.2	~ 49 [f]	-0.26	4
Gold electrode [d]	11.7	/	/	4
Silver electrode [d]	11.1	/	/	4
SS electrode (SUS 304)	6.7	~ 21 [f]	-0.55	4
3D macroporous on SS fiber felt	6.1	/	/	23
Nickel electrode [d]	3.8	~ 135 [f]	-0.21	4
CNTs-stainless steel mesh	3.6	/	/	24
Surface oxygen-rich titanium	~ 0	/	/	12
Titanium electrode [d]	~ 0	/	/	4
Titanium plate (TNs)	12.7	~ 30 [g]	-0.08	*
Untreated graphite felt	11.3	~ 25-75 [e]	/	*

(a) Projected surface area current density; (b) Prices are given per cubic metres of electrode; (c) The corrosion potential was recorded by LSV in sterile M9 solution (Fig. S8); (d) Metal power was formed into platelike electrode by extrusion; (e) Values of stainless steel electrode substrate from Ref 25; (f) Values of those metal electrode substrate from Ref 4; (g) Values of titanium plate (approximately pure metal) form Argus metals (https://www.metalprices.com/)

* This study

336